

# Molecular Structure Theory without the Born–Oppenheimer Approximation: Rotationless Vibrational States of LiH

Published as part of *The Journal of Physical Chemistry A* special issue “Rodney J. Bartlett Festschrift”.

Saeed Nasiri,\* Sergiy Bubin,\* Monika Stanke,\* and Ludwik Adamowicz\*



Cite This: *J. Phys. Chem. A* 2024, 128, 9175–9183



Read Online

ACCESS |



Metrics & More

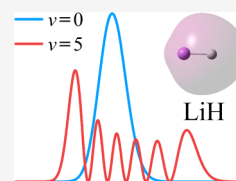


Article Recommendations



Supporting Information

**ABSTRACT:** Low-lying rotationless states of the lithium hydride molecule are studied in the framework of the variational method without assuming the Born–Oppenheimer (BO) approximation. Highly accurate solutions to the six-particle (two nuclei and four electrons) Schrödinger equation are obtained by means of expanding the wave functions of the considered states in terms of many thousands of all-particle explicitly correlated Gaussians. The basis functions are optimized independently for each state using the analytic energy gradient with respect to the nonlinear parameters. The non-BO wave functions obtained in the calculations are used to evaluate the leading-order relativistic and quantum electrodynamics energy corrections in the framework of the perturbation theory. The geometric structure of the molecule in the ground and excited states is discussed based on the analysis of the nucleus–nucleus correlation functions. The non-BO energies and structural parameters obtained of this work are compared with the most accurate BO results currently available.



## INTRODUCTION

The accuracy of the quantum-mechanical calculations of molecular stationary states depends on several factors, the most important of which is how close the multiparticle functional basis set used in the calculations is to being complete. Since the particles that make up a molecule, electrons and nuclei, have very different masses, it is generally possible to reduce the complexity of the original quantum-mechanical problem by separating particles into fast and slow ones. In this process, one solves the Schrödinger equation to determine the electronic wave function and the corresponding electronic energy at some selected geometries of the molecule and generates a potential energy surface (PES), which is subsequently used to determine stationary states associated with the rovibrational motion of the nuclei in the molecule. This separation constitutes one of the pillars of modern quantum chemistry—the Born–Oppenheimer approximation. In most PES calculations the electronic wave function is expanded in terms of Slater determinants (configurations) formed using a set of molecular orbitals (MOs) that usually are linear combinations of single-electron atomic orbitals. The accuracy of the calculation mainly depends on the completeness of the configuration space and the completeness of molecular-orbital space. However, in some cases small or not-so-small inaccuracy may also come from the separation of the electronic and nuclear motions.

Let us start with some general comments concerning our development works of methods that aim at increasing the completeness of the configuration and orbital manifolds for the electronic problem. To make the configuration space more complete we implemented the complete single-reference coupled cluster (CC) method with single, double, triple, and quadruple excitations (CCSDTQ)<sup>1</sup> and a multireference

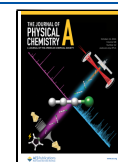
coupled cluster method with the complete-active-space (CAS) reference wave function—the CASCC method.<sup>2–4</sup> Both methods are rigorously size extensive. To increase the completeness of the molecular-orbital space for single- and multireference coupled cluster calculations we have introduced two methods. In the first method, applicable to atomic and diatomic systems, numerical orbitals generated for every electron-pair in the system using a numerical-orbital multi-configuration self-consistent field procedure (MCSCF) are combined to form a basis set for the CC calculation.<sup>5–11</sup> The second method involves generating a set of virtual orbitals (VOs) in an SCF calculation (RHF or UHF) using an extended atomic-orbital basis set, than partitioning this set into a smaller set of active VOs and a set of inactive VOs, and using the second-order correlation Hylleraas functional to mix the active VOs with the inactive VOs with a unitary transformation matrix whose matrix elements are determined by the minimization of the Hylleraas functional determined using only the active VOs.<sup>12–21</sup> Subsequently, the optimized active RHF (or UHF) VOs (also called the first-order correlation orbitals) are used to perform the CC calculation. Thus, an extended atomic basis set can be used in the calculation because the post-SCF calculation is performed not with all SCF virtual orbitals, but with a much smaller set of the active VOs. A procedure has also implemented for the zero-

Received: July 5, 2024

Revised: August 26, 2024

Accepted: August 30, 2024

Published: October 12, 2024



order wave function being an MCSCF wave function<sup>22</sup> and for generating active VOs that are optimized for the contributions of the double excitations, as well as the single excitations, to the wave function. In the latter case the fourth-order Hylleraas functional is used.<sup>23</sup>

The accuracy one can achieve with an orbital-based methods, even if the methods are rigorously size-extensive and highly configurationally complete, and even if a very large set of atomic orbital is used, is somewhat limited. The results for such properties as, for example, interstate transition energies, are not as accurate as the state-of-the-art high-resolution spectroscopic measurements. To achieve or even to exceed the ever increasing accuracy of the experimental spectroscopy one needs to employ a method that is capable of almost exactly account for the electron-correlation effects in the system. For small molecular systems with 2–4 nuclei and with up to 5–6 electrons, and for small atoms with up to 6–7 electrons this can currently be achieved only by expanding the wave functions of the considered states of the system in terms of all-particle explicitly correlated basis functions (ECBF), i.e., the basis functions that explicitly depend on the interparticle distances. While in the BO ECBF molecular calculations the basis functions only depend on the coordinates of the electrons, in the non-BO calculations, where all particles are treated on an equal footing, they depend on the coordinates of both the electrons and nuclei. The non-BO calculations are more intricate than the BO calculations, as in the latter ones the wave function not only represents the quantum state of the electrons, but also describes the motion of the system's nuclei. In our works we have used various forms of all-particle explicitly correlated Gaussian functions (ECGs) in atomic and molecular BO and non-BO molecular calculations.<sup>24–27</sup> As the Hamiltonian used in the atomic and molecular non-BO calculations that represents the internal motion of the system is isotropic (i.e., invariant with respect to 3D rotations) these functions should provide basis sets for irreducible representations of the SO(3) group. The ECGs used in this work for expanding the wave functions of the ground and excited states corresponding to the zero total orbital angular quantum number are such functions. In the present work we present an example of high-precision non-BO ECG calculations performed for the lowest nine states of the lithium hydride (LiH) molecule that correspond to the zero total orbital angular momentum of the molecule (i.e., the angular momentum associated with the rotational motion of the electrons and the nuclei). We nominally call these states rotationless vibrational states even though, strictly speaking, the vibrational quantum number is not a good quantum number to label energies and the corresponding wave functions obtained by solving the time-independent Schrödinger equation for all particles. The reason for it not being a good quantum number is the nonadiabatic coupling of the vibrational motion of the nuclei and the motion of the electrons. They are directly accounted for in the all-particle non-BO Hamiltonian that represents the motion of the electrons and the motion of the nuclei in the system. Despite the inexactness of the term “vibrational states” it will be used in the further discussion in the present work because of the lack of a better term.

The LiH calculations presented in this work are the largest high-precision non-BO molecular calculations for the ground and excited states of a molecular system performed to date. LiH, despite its seemingly straightforward electronic structure, continues to captivate researchers in the field of quantum chemistry. Its importance extends across various scientific domains, driven by several compelling factors. With only four

electrons, LiH serves as an ideal benchmark for assessing the accuracy and reliability of new computational methods. LiH molecule is often used as a reference system to validate data obtained from emerging techniques, ensuring their correctness. Over recent decades, LiH has gained significance in both chemistry and physics. The molecule features prominently in theoretical studies, particularly regarding its bonding nature. However, due to inherent approximations, results from different methods occasionally diverge. The significance of the LiH molecule has made it a subject of several theoretical investigations employing ECG basis functions over the past decades. Highly accurate nonrelativistic energies have been obtained, both within the framework of the BO approximation<sup>28–30</sup> and beyond the BO approximation.<sup>31,32</sup>

On the experimental side, LiH's observation in the center of the galaxy has captured the attention of astrophysicists. This cosmic context adds to its scientific allure. Furthermore, the ever improving precision of measurement techniques provides increasingly accurate electronic structure data. For this reason computational chemists and physicists are compelled to enhance the precision of their calculations.

## METHODS

The approach used in this work to calculate the lowest nine rotationless vibrational states of the LiH molecule was described in our previous papers.<sup>31–33</sup> Let us only briefly summarize the major features of the method. The following nonrelativistic internal Hamiltonian is used in the present calculations:

$$\mathcal{H}_{\text{nr}}^{\text{int}} = -\frac{1}{2} \left( \sum_{i=1}^n \frac{1}{\mu_i} \nabla_{\mathbf{r}_i}^2 + \sum_{i=1}^n \sum_{j \neq i}^n \frac{1}{m_0} \nabla_{\mathbf{r}_i} \nabla_{\mathbf{r}_j} \right) + \sum_{i=1}^n \frac{q_0 q_i}{r_i} + \sum_{i=1}^n \sum_{j < i}^n \frac{q_i q_j}{r_{ij}} \quad (1)$$

where  $n = N - 1$  with  $N$  being the total number of particles in the molecule (e.g., the sum of the number of the nuclei and the number of electrons;  $N = 6$  for LiH),  $m_0$  is the mass of the reference nucleus ( ${}^7\text{Li}$ ,  $m_0 = 12786.392282 m_e$ <sup>34</sup>) and  $q_0$  is its charge,  $q_i$ ,  $i = 1, \dots, n$ , are the charges of the other particles,  $\mu_i = m_0 m_i / (m_0 + m_i)$  is the reduced mass of particle  $i$  ( $m_i$ ,  $i = 1, \dots, n$ , are the particle masses),  $r_i$ ,  $i = 1, \dots, n$  is the distance from particle  $n + 1$  to the reference particle, i.e., particle 1, and  $r_{ij}$  is the distance between particle  $j + 1$  and particle  $i + 1$ . The prime symbol in eq 1 denotes the matrix/vector transposition. The internal Hamiltonian describes the motion of  $n$  particles whose charges are the charges of the original particles but their masses are changed to the corresponding reduced masses. We refer to these particles as “pseudoparticles”. They move in the central field created by the charge of the reference nucleus. The internal Hamiltonian is invariant upon all rotations about the center of the internal coordinate system and one can think of it as an “atom-like” Hamiltonian. The eigenfunctions of this Hamiltonian can be classified using the same symmetries as the wave functions of an atom. These eigenfunctions and the corresponding eigenvalues (energies) represent all modes of the internal motions of the molecule including the electronic, vibrational, and rotational motions. In particular, the ground-state solution is spherically symmetric, i.e., it is invariant under 3D rotations.

Hamiltonian (1) can also be conveniently written in the matrix form:<sup>35</sup>

$$\mathcal{H}_{\text{nr}} = -\nabla_r' \mathbf{M} \nabla_r + \sum_{i=1}^5 \frac{q_0 q_i}{r_i} + \sum_{i=1}^5 \sum_{j<i}^5 \frac{q_i q_j}{r_{ij}} \quad (2)$$

where for LiH

$$\nabla_r = \begin{pmatrix} \nabla_{r_1} \\ \vdots \\ \nabla_{r_5} \end{pmatrix}$$

is a 15-component column gradient vector, and  $\mathbf{M} = M \otimes \mathbf{I}$  is the Kronecker product of a  $5 \times 5$  matrix  $M$  and the  $3 \times 3$  identity matrix  $\mathbf{I}$ . The diagonal elements of matrix  $M$  are  $1/(2\mu_1), \dots, 1/(2\mu_5)$ , while all off-diagonal elements are equal to  $1/(2m_0)$ .

In order to obtain accurate eigenvalues and wave functions corresponding to rotationless states of Hamiltonian (2), we expand the wave functions in terms of spherically symmetric all-electron explicitly correlated Gaussian (ECG) basis functions, which have the following form:

$$\phi_k = r_1^{m_k} \exp[-r'(A_k \otimes \mathbf{I})r] \quad (3)$$

where  $r_1$  is the distance between the nuclei,  $m_k$  is an even integer (in this work,  $m_k$  is constrained within the range 0–200 and it is regarded as an integer variational parameter), and  $A_k$  is an  $n \times n$  real symmetric matrix of the exponential variational parameters. Note that both  $A_k$  and  $m_k$  are unique and independently tunable for each basis function, which is indicated by the presence of index  $k$ . Vector  $r$  in eq 3 is a  $3n$ -component vector formed by stacking the internal Cartesian coordinates,  $r_i$ :

$$r = \begin{pmatrix} r_1 \\ r_2 \\ \vdots \\ r_n \end{pmatrix} \quad (4)$$

Let us denote  $A_k = A_k \otimes \mathbf{I}$ . Matrix  $A_k$  and, by extension,  $A_{k'}$  have to be positive definite in order for Gaussian basis function (3) to be square integrable. To ensure positive definiteness of  $A_k$  we adopt the following Cholesky-factored form for it:  $A_k = (L_k L_k') \otimes \mathbf{I}$ , where  $L_k$  is a  $n \times n$  lower-triangular matrix of real numbers. In this representation,  $A_k$  is automatically positive definite for any real-valued  $L_k$ . The elements of matrix  $L_k$  are variational parameters that are thoroughly optimized in the present calculations. The optimization employs the analytical energy gradient determined with respect to the  $L_k$  matrix elements. The optimization is carried independently for each considered state.

All present calculations are performed using our in-house parallel computer code written in Fortran and employing MPI (Message Passing Interface) for communication between parallel processes. It should be noted that the generation of the basis set for each considered state is by far the most time-consuming step of the calculations. It has required well over a year of continuous computing using several hundred cores on parallel computer systems equipped with x86 central processing units. The parameters of the generated basis sets for all considered states in this work are available in the [Supporting Information](#). The need for inclusion of  $r_1^{m_k}$  factors in Gaussian basis functions can be explained by analyzing the internal Hamiltonian. Specifically, within the context of  $\mathcal{H}_{\text{nr}}$ , pseudoparticle 1 represents the proton. Consequently, a significant Coulombic repulsion arises between this proton and the charge

of the lithium nucleus located at the center of the internal coordinate system. The pair correlation function between the two nuclei, which depends on the internuclear distance  $r_1$ , must rapidly approach zero as  $r_1$  approaches zero. Conversely, for a diatomic molecule in the ground state, this pair correlation function exhibits a pronounced peak around  $r_1 \approx r_e$ , where  $r_e$  is the equilibrium bond length of the molecule. In the case of vibrationally excited states, the corresponding pair correlation function displays multiple radial peaks, all distinct from the origin at  $r_1 = 0$ . Given that an origin-centered Gaussian function achieves its maximum at  $r_1 = 0$ , it necessitates shifting the Gaussian maximum away from coordinate center. However, this shifting has to be done in a spherically symmetric manner so that the spherical symmetry of the Gaussian is not broken. For the basis functions used in this work, the adjustment is achieved by introducing the  $r_1^{m_k}$  preexponential factors, which not only displace the Gaussian maxima away from the origin but also allows to describe the radial oscillations of the wave functions that correspond to vibrational excited states.

The present calculations concern the ground and lowest nine vibrational excited singlet states of the LiH molecule. In constructing the wave functions for these states, the proper permutational symmetry of the electrons is taken into account. This is achieved using the spin-free formalism.<sup>36–38</sup> The key element of this formalism is the construction of an appropriate permutational symmetry projector,  $\mathcal{Y}$ . The action of this projector on each basis function yields a combination of Gaussians which are used to calculate the Hamiltonian and overlap matrix elements. These terms can be equivalently generated by combining the (spatial) basis functions with the appropriate spin components and summing over the electronic spin coordinates. By applying projector  $\mathcal{Y}$  to each basis function the desired permutational symmetry is implemented. For the LiH molecule with four electrons (labeled as particles 3, 4, 5, and 6; particle 1 is the Li nucleus and particle 2 is the proton) in a singlet state the  $\mathcal{Y}$  operator has the following form in terms of the labels of the original particles:

$$\mathcal{Y} = (1 + \mathcal{P}_{34})(1 + \mathcal{P}_{56})(1 - \mathcal{P}_{35})(1 - \mathcal{P}_{46}) \quad (5)$$

where permutations  $\mathcal{P}_{ij}$  exchange the indices of electrons  $i$  and  $j$ . As the internal Hamiltonian and, consequently, the wave function depend not on the coordinates of the original particles, but on the coordinates of the pseudoparticles, i.e., on the internal coordinates,  $\mathcal{Y}$  needs to be first expressed in terms of the pseudoparticle labels before it is applied to the basis functions.

The first step of the present calculations involves determining the nonrelativistic non-BO energies and the corresponding nonrelativistic wave functions of the considered states. Even though these calculations are very precise and very well converged, they would fall short in accurately determining the total energies and the interstate transition energies when compared to the state-of-the-art spectroscopic measurements. To achieve better agreement with experiment, one needs to account for the relativistic and QED energy corrections in the calculations. In practice, accounting for these effects involve expanding the total energy of the studied system in a series in terms of powers of the fine-structure constant,  $\alpha$ :<sup>39,40</sup>

$$E_{\text{tot}} = E_{\text{nr}} + \alpha^2 E_{\text{rel}}^{(2)} + \alpha^3 E_{\text{QED}}^{(3)} + \dots \quad (6)$$

**Table 1.** Convergence of the Nonrelativistic Variational Non-BO Energy ( $E_{\text{nr}}$ ) and the Expectation values of the Mass–Velocity Hamiltonian ( $\mathcal{H}_{\text{MV}}$ ), Orbit–Orbit Hamiltonian ( $\mathcal{H}_{\text{OO}}$ ), and One- and Two-electron Dirac  $\delta$ -functions for the Lowest Nine Vibrational States of the LiH Molecule<sup>a</sup>

State	Basis	$E_{\text{nr}}$	$\langle \mathcal{H}_{\text{MV}} \rangle$	$\langle \mathcal{H}_{\text{OO}} \rangle$	$\langle \delta(\mathbf{r}_{\text{e}}) \rangle$	$\langle \delta(\mathbf{r}_{\text{H-e}}) \rangle$	$\langle \delta(\mathbf{r}_{\text{e-e}}) \rangle$
$\nu = 0$	13 000	−8.06643893	−79.05380	−0.4730653	3.451749	0.095057	0.09164891
	15 000	−8.06643902	−79.06215	−0.4730649	3.452126	0.095078	0.09164623
	17 000	−8.06643920	−79.06261	−0.4730611	3.452145	0.095099	0.09164556
	$\infty$	−8.06643939(20)	−79.06315(54)	−0.4730560(51)	3.452171(26)	0.095126(27)	0.09164503(54)
$\nu = 1$	13 000	−8.06024309	−79.0284	−0.4724645	3.45088	0.094253	0.09157994
	15 000	−8.06024336	−79.0291	−0.4724673	3.45093	0.094263	0.09156291
	17 000	−8.06024379	−79.0325	−0.4724724	3.45113	0.094273	0.09155992
	$\infty$	−8.06024420(41)	−79.0368(43)	−0.4724793(68)	3.45138(26)	0.094287(14)	0.0915570(29)
$\nu = 2$	13 000	−8.0542462	−78.9958	−0.471586	3.44962	0.09343	0.091533
	15 000	−8.0542504	−78.9971	−0.471594	3.44972	0.09344	0.091526
	17 000	−8.0542521	−79.0003	−0.471600	3.44989	0.09358	0.091515
	$\infty$	−8.0542538(17)	−79.0046(43)	−0.471609(83)	3.45010(21)	0.09377(19)	0.091504(11)
$\nu = 3$	13 000	−8.0484472	−78.9724	−0.470175	3.44848	0.09249	0.091529
	15 000	−8.0484564	−78.9783	−0.470276	3.44912	0.09252	0.091503
	17 000	−8.0484596	−78.9828	−0.470311	3.44942	0.09260	0.091467
	$\infty$	−8.0484636(40)	−78.9888(60)	−0.470357(46)	3.44983(41)	0.09272(11)	0.091427(40)
$\nu = 4$	13 000	−8.0428375	−78.9293	−0.46775	3.44672	0.091755	0.091515
	15 000	−8.0428560	−78.9352	−0.46801	3.44720	0.091776	0.091500
	17 000	−8.0428619	−78.9381	−0.46813	3.44742	0.091803	0.091462
	$\infty$	−8.0428687(68)	−78.9422(40)	−0.46828(16)	3.44769(28)	0.091816(13)	0.091450(12)
$\nu = 5$	13 000	−8.037412	−78.9150	−0.46528	3.44584	0.09108	0.091501
	15 000	−8.037445	−78.9257	−0.46574	3.44671	0.09112	0.091475
	17 000	−8.037456	−78.9256	−0.46601	3.44697	0.09126	0.091445
	$\infty$	−8.037470(14)	−78.9282(26)	−0.46640(38)	3.44730(34)	0.09147(20)	0.091428(17)
$\nu = 6$	13 000	−8.032158	−78.8748	−0.46679	3.44417	0.090325	0.091410
	15 000	−8.032216	−78.8830	−0.46694	3.44490	0.090407	0.091360
	17 000	−8.032236	−78.8878	−0.46703	3.44537	0.090454	0.091316
	$\infty$	−8.032259(24)	−78.8945(67)	−0.46715(12)	3.44599(62)	0.090515(61)	0.091264(52)
$\nu = 7$	13 000	−8.027067	−78.8498	−0.46636	3.44286	0.08952	0.091453
	15 000	−8.027168	−78.8547	−0.46649	3.44363	0.08968	0.091378
	17 000	−8.027200	−78.8584	−0.46658	3.44401	0.08977	0.091338
	$\infty$	−8.027238(38)	−78.8637(53)	−0.46671(13)	3.44458(57)	0.08991(14)	0.091320(18)
$\nu = 8$	13 000	−8.022126	−78.8203	−0.46566	3.44087	0.088784	0.091444
	15 000	−8.022294	−78.8297	−0.46580	3.44244	0.088882	0.091379
	17 000	−8.022337	−78.8369	−0.46587	3.44300	0.088973	0.091336
	$\infty$	−8.022383(46)	−78.8463(94)	−0.46597(10)	3.44376(76)	0.089097(12)	0.091288(48)

<sup>a</sup>Results obtained with basis sets of different size are shown along with the extrapolated values. The numbers in parentheses are estimated uncertainties of the extrapolation due to the basis set truncation. All values are in a.u.

where  $E_{\text{nr}}$  is the nonrelativistic energy of the considered state of the system, the second term,  $\alpha^2 E_{\text{rel}}^{(2)}$ , represents the leading-order relativistic correction, the third term  $\alpha^3 E_{\text{QED}}^{(3)}$  represents the leading-order QED correction, and so on. Each of these terms is evaluated as an expectation value of a certain effective Hamiltonian. In our calculations, quantity  $E_{\text{rel}}^{(2)}$  in eq 6 is the expectation value of the Breit-Pauli Hamiltonian,  $\mathcal{H}_{\text{rel}}$ , corresponding to the singlet state.<sup>41,42</sup> In the present work,  $\mathcal{H}_{\text{rel}}$ , before it is used in the calculations, is expressed in terms of the internal coordinates. The mass–velocity term ( $\mathcal{H}_{\text{MV}}$ ), the Darwin term ( $\mathcal{H}_{\text{D}}$ ), the orbit–orbit interaction term ( $\mathcal{H}_{\text{OO}}$ ), and the spin–spin Fermi contact interaction term ( $\mathcal{H}_{\text{SS}}$ ) are included in  $\mathcal{H}_{\text{rel}}$ :

$$\mathcal{H}_{\text{rel}} = \mathcal{H}_{\text{MV}} + \mathcal{H}_{\text{D}} + \mathcal{H}_{\text{OO}} + \mathcal{H}_{\text{SS}} \quad (7)$$

The explicit expressions for the corresponding effective operators in the internal coordinates are as follows:<sup>55,43</sup>

$$\mathcal{H}_{\text{MV}} = -\frac{1}{8} \left[ \frac{1}{m_0^3} \left( \sum_{i=1}^n \nabla_{\mathbf{r}_i} \right)^4 + \sum_{i=1}^n \frac{1}{m_i^3} \nabla_{\mathbf{r}_i}^4 \right] \quad (8)$$

$$\mathcal{H}_{\text{D}} = -\frac{\pi}{2} \left[ \sum_{i=2}^n \frac{q_0 q_i}{m_i^2} \delta(\mathbf{r}_i) + \sum_{i=2}^n \frac{q_1 q_i}{m_i^2} \delta(\mathbf{r}_{1i}) + \sum_{\substack{i,j=2 \\ i \neq j}}^n \frac{q_i q_j}{m_i^2} \delta(\mathbf{r}_{ij}) \right] \quad (9)$$

**Table 2.** Comparison of the Calculated and Experimentally Derived  $\nu + 1 \rightarrow \nu$  ( $\nu = 0 \dots 7$ ) Transition Energies ( $\Delta E$ ) for the Rovibrational States of LiH.<sup>a</sup>

Method	$\Delta E_{\text{nr}}$	$\Delta E_{\text{nr+rel}}$	$\Delta E_{\text{nr+rel+QED}}$	Method	$\Delta E_{\text{nr}}$	$\Delta E_{\text{nr+rel}}$	$\Delta E_{\text{nr+rel+QED}}$
1 $\rightarrow$ 0				2 $\rightarrow$ 1			
non-BO-ECG	1359.681(53)	1359.73(53)	1359.725(53)	non-BO-ECG	1314.83(20)	1314.90(18)	1314.889(18)
BO-ECG <sup>28,b</sup>	1359.77			BO-ECG <sup>28,b</sup>	1314.90		
BO-FCI <sup>49,c</sup>	1359.66			BO-FCI <sup>49,c</sup>	1314.68		
MR-CISD <sup>50,d</sup>	1360.63			MR-CISD <sup>50,d</sup>	1315.58		
Experiment <sup>51,e</sup>			1359.71(2)	Experiment <sup>51,e</sup>			1314.89(2)
Experiment <sup>52,f</sup>			1359.7085(20)	Experiment <sup>52,f</sup>			1314.8518(20)
3 $\rightarrow$ 2				4 $\rightarrow$ 3			
non-BO-ECG	1271.13(18)	1271.17(18)	1271.16(18)	non-BO-ECG	1228.28(28)	1228.33(27)	1228.31(28)
BO-ECG <sup>28,b</sup>	1270.97			BO-ECG <sup>28,b</sup>	1227.86		
BO-FCI <sup>49,c</sup>	1270.55			BO-FCI <sup>49,c</sup>	1227.31		
MR-CISD <sup>50,d</sup>	1271.46			MR-CISD <sup>50,d</sup>	1228.19		
Experiment <sup>51,e</sup>			1270.89(2)	Experiment <sup>51,e</sup>			1227.77(2)
Experiment <sup>52,f</sup>			1270.9098(20)	Experiment <sup>52,f</sup>			1227.8061(20)
5 $\rightarrow$ 4				6 $\rightarrow$ 5			
non-BO-ECG	1185.73(79)	1185.77(78)	1185.77(77)	non-BO-ECG	1144.5(12)	1144.41(2)	1144.4(12)
BO-ECG <sup>28,b</sup>	1185.51			BO-ECG <sup>28,b</sup>	1143.80		
BO-FCI <sup>49,c</sup>	1184.87			BO-FCI <sup>49,c</sup>	1143.06		
MR-CISD <sup>50,d</sup>	1185.70			MR-CISD <sup>50,d</sup>	1143.86		
Experiment <sup>51,e</sup>			1185.44(2)	Experiment <sup>51,e</sup>			1143.77(2)
Experiment <sup>52,e</sup>			1185.4519(20)	Experiment <sup>52,f</sup>			1143.7438(20)
7 $\rightarrow$ 6				8 $\rightarrow$ 7			
non-BO-ECG	1102.9(21)	1103.0(21)	1103.0(21)	non-BO-ECG	1064.5(28)	1064.6(28)	1064.5(28)
BO-ECG <sup>28,b</sup>	1102.62			BO-ECG <sup>28,b</sup>	1061.83		
BO-FCI <sup>49,c</sup>	1101.72			BO-FCI <sup>49,c</sup>	1060.73		
MR-CISD <sup>50,d</sup>	1102.58			MR-CISD <sup>50,d</sup>	1061.69		
Experiment <sup>51,e</sup>			1102.60(2)	Experiment <sup>51,e</sup>			1061.78(2)
Experiment <sup>52,g</sup>			1102.57(7)	Experiment <sup>52,g</sup>			1061.76(15)

<sup>a</sup>Results obtained in the present work are extrapolated to the infinite basis set limit and labeled as non-BO-ECG. All values are in  $\text{cm}^{-1}$ . <sup>b</sup>BO calculations with 2400 ECG basis functions. <sup>c</sup>Full Configuration-Interaction/(42s18p10d). <sup>d</sup>The internally contracted configuration interaction in the single and double space (MR-CISD) level with four electrons distributed among the five orbitals arising from the 1s, 2s, and 2p atomic orbitals in the multiconfigurational self-consistent-field (MCSCF) part of the calculations are used. <sup>e</sup>The original published data does not contain uncertainties. The uncertainty was estimated by the current authors. <sup>f</sup>The original published data does not contain uncertainties. We estimated the uncertainties based on the employed experimental data for the ground electronic  $X$  state in the fitting procedure. <sup>g</sup>The original published data does not contain uncertainties. We estimated the uncertainties based on the uncertainty of the employed experimental data (the vibrationaly-resolved transition between the ground electronic  $X$  state and first electronic excited  $A$  state) in the fitting procedure.

$$\mathcal{H}_{\text{OO}} = -\frac{1}{2} \sum_{i=1}^n \sum_{j=1}^n \frac{q_i q_j}{m_i m_j} \left[ \frac{1}{r_j} \nabla'_i \nabla_j + \frac{1}{r_j^3} \mathbf{r}'_j (\mathbf{r}'_j \nabla'_i) \nabla_j \right] + \frac{1}{2} \sum_{i=1}^n \sum_{j>i}^n \frac{q_i q_j}{m_i m_j} \left[ \frac{1}{r_{ij}} \nabla'_i \nabla_j + \frac{1}{r_{ij}^3} \mathbf{r}'_{ij} (\mathbf{r}'_{ij} \nabla'_i) \nabla_j \right], \quad (10)$$

and

$$\mathcal{H}_{\text{SS}} = -\frac{8\pi}{3} \sum_{i,j=2}^5 \frac{q_i q_j}{m_i m_j} (\mathbf{s}'_i \mathbf{s}'_j) \delta(r_{ij}), \quad (11)$$

where in the last expression,  $\mathbf{s}_i$  denotes the spin operator of the  $i$ -th pseudoparticle. For LiH in a singlet state,  $\mathbf{s}'_i \mathbf{s}'_j = -3/4$ . The relativistic corrections for a particular state are calculated as the expectation values of the above operators using the state's nonrelativistic non-BO wave function.

The largest contribution to the leading QED correction arises from the term which includes the so-called Bethe logarithm,  $\ln k_0$ .<sup>44,45</sup> In our previous work,<sup>31</sup> we discussed the challenges

associated with computing this QED correction. The primary difficulty lies in accurately determining the term involving  $\ln k_0$ . To our knowledge, no direct calculation of  $\ln k_0$  for the LiH molecule has been reported. However, it is known that the dominant contribution to  $\ln k_0$  in atoms arises from the inner shell electrons. Therefore, one can adopt the following approximate expression for the effective leading-order QED Hamiltonian:

$$\mathcal{H}_{\text{QED}}^{(3)} \approx \frac{4q_0}{3} \left( \frac{19}{30} - 2 \ln \alpha - \ln k_0(\text{Li}) \right) \left\langle \sum_{i=2}^5 \delta(r_{\text{Li}-i}) \right\rangle + \frac{4q_{\text{H}}}{3} \left( \frac{19}{30} - 2 \ln \alpha - \ln k_0(\text{H}) \right) \left\langle \sum_{i=2}^5 \delta(r_{\text{H}-i}) \right\rangle \quad (12)$$

where  $\ln k_0(\text{Li}) = 5.178080$  and  $\ln k_0(\text{H}) = 2.984129$  are the Bethe logarithm values for the Li and H atoms, respectively.<sup>46,47</sup>

Equations 8, 9, 11, and 12 contain singular operators, namely the fourth powers of the linear momenta and Dirac delta functions, whose expectation values are known to exhibit somewhat slower convergence with the basis size compared to

**Table 3.** Expectation Values of the Interparticle Distances  $r_i$  and  $r_{ij}$  as well as their Squares for the Lowest Rotationless States of LiH Obtained in this Work (Values Extrapolated to the Infinite Basis Set Limit are Shown)<sup>a</sup>

Quantity	Method	$\nu = 0$	$\nu = 1$	$\nu = 2$	$\nu = 3$	$\nu = 4$
$\langle r_{\text{Li-H}} \rangle$	non-BO-ECG	3.06103685(61)	3.1549895(37)	3.2512667(11)	3.3500062(69)	3.451386(25)
$\langle r_{\text{Li-H}} \rangle$	BO-ECG <sup>28,b</sup>	3.06029188	3.15422580	3.25046745	3.34916919	3.45050556
$\langle r_{\text{Li-H}} \rangle$	MRCISD <sup>53,c</sup>	3.01901570				
$r_e$	Fitting <sup>51</sup>	3.015217				
$r_e$	Fitting <sup>52,d</sup>	3.01523597				
$r_e$	Fitting <sup>54,e</sup>	3.01394640				
$\langle r_{\text{Li-e}} \rangle$	non-BO-ECG	1.97193294(25)	2.0070042(16)	2.04291183(43)	2.0796617(30)	2.1172597(65)
$\langle r_{\text{H-e}} \rangle$	non-BO-ECG	2.56510469(25)	2.6242863(25)	2.6851230(32)	2.7477748(66)	2.812442(20)
$\langle r_{\text{e-e}} \rangle$	non-BO-ECG	2.95593984(31)	3.0087987(28)	3.0631229(15)	3.1189796(27)	3.1764480(98)
$\langle r_{\text{Li-H}}^2 \rangle$	non-BO-ECG	9.4197074(62)	10.104694(38)	10.8261936(45)	11.586883(84)	12.38962(27)
$\langle r_{\text{Li-e}}^2 \rangle$	non-BO-ECG	6.5857432(14)	6.866602(15)	7.160562(10)	7.468172(22)	7.790007(73)
$\langle r_{\text{H-e}}^2 \rangle$	non-BO-ECG	7.7452174(12)	8.171204(17)	8.621241(27)	9.097530(43)	9.602690(65)
$\langle r_{\text{e-e}}^2 \rangle$	non-BO-ECG	10.9660723(27)	11.394848(27)	11.844963(31)	12.317734(27)	12.81476(11)
Quantity	Method	$\nu = 5$	$\nu = 6$	$\nu = 7$	$\nu = 8$	
$\langle r_{\text{Li-H}} \rangle$	non-BO-ECG	3.555642(25)	3.663227(88)	3.77388(30)	3.88912(24)	
$\langle r_{\text{Li-H}} \rangle$	BO-ECG <sup>28,b</sup>	3.55471135	3.66206834	3.77288418	3.88765124	
$\langle r_{\text{Li-e}} \rangle$	non-BO-ECG	2.155738(16)	2.195150(28)	2.235335(98)	2.276832(73)	
$\langle r_{\text{H-e}} \rangle$	non-BO-ECG	2.879364(16)	2.949006(89)	3.02162(18)	3.09770(18)	
$\langle r_{\text{e-e}} \rangle$	non-BO-ECG	3.235661(39)	3.296795(80)	3.35999(18)	3.42548(27)	
$\langle r_{\text{Li-H}}^2 \rangle$	non-BO-ECG	13.23822(59)	14.13675(27)	15.0872(31)	16.10223(51)	
$\langle r_{\text{Li-e}}^2 \rangle$	non-BO-ECG	8.12674(11)	8.47951(24)	8.8473(11)	9.2365(11)	
$\langle r_{\text{H-e}}^2 \rangle$	non-BO-ECG	10.14030(30)	10.71460(52)	11.3312(20)	11.9953(23)	
$\langle r_{\text{e-e}}^2 \rangle$	non-BO-ECG	13.337795(90)	13.89030(72)	14.4742(18)	15.0921922(18)	

<sup>a</sup>For comparison we also present vibrationally averaged bond lengths reported in some BO calculations ( $\langle r_{\text{Li-H}} \rangle$ ) and the “experimental” equilibrium bond lengths determined by fitting the potential energy curve using the existing spectroscopic data for LiH ( $r_e$ ). All values are in a.u. <sup>b</sup>BO calculations with 2400 ECG basis functions. <sup>c</sup>Internally contracted configuration interaction calculations with single and double excitations (MRCISD) from configurations obtained by distributing four electrons among five active orbitals (MRCISD+Q) arising from the 1s, 2s, and 2p atomic orbitals in the multiconfigurational self-consistent-field (MCSCF) part of the calculations were used. <sup>d</sup>Direct least-squares fit of the effective potential energy, Born-Oppenheimer breakdown (BOB) and J-independent non-adiabatic functions to experimental data were used. <sup>e</sup>Inversion of the BOB corrections procedure were used in the least-squares fit.

the nonsingular ones (e.g., nonrelativistic Hamiltonian). In this work all these expectation values are evaluated directly, i.e., without invoking any regularization technique. However, the resulting accuracy is still sufficient for the purpose of this work.

## RESULTS AND DISCUSSION

Table 1 shows the results of the calculations of the total non-BO nonrelativistic energies, and leading relativistic corrections, and some key expectation values for the LiH molecule in the lowest nine vibrational states ( $\nu = 0 - 8$ ). The results shown in the table are obtained with the basis set sizes that increase from 13 000 to 17 000. The energies and the other expectation values are extrapolated to the infinite basis set size limit. Our experience with ECG calculations over the past two decades indicates that the increments of the energy (and some other properties) obtained when the basis is extended by a certain number of functions often exhibit a pattern that is similar to a geometric progression. Therefore, our extrapolation to the infinite basis set size limit is based on the geometric progression approximation. For more information, please see our previous paper.<sup>48</sup>

The extrapolated values are shown in the table along with the corresponding estimated uncertainties. As one can see, all LiH expectation values are relatively well converged. However, as expected, the convergence rate is better for the lower states than for the higher ones. The basis sets used to obtain the results in

Table 1 are generated in a process that begins with a small set of Gaussian functions, whose nonlinear parameters are selected using a mix of random and physically motivated choices and then optimized. Subsequently, the basis set is expanded in several steps. In each step, new Gaussian functions are added and variationally optimized using a procedure that employs the analytical energy gradient. The enlargement and subsequent optimization are done using a one-function-at-a-time approach. After a newly added function is optimized, it is checked for linear dependency (within a predefined threshold) with the functions already included in the set. If no linear dependency is detected, the function is included in the basis set. As mentioned previously, both the  $L_k$  matrix elements and the  $m_k$  powers in the  $r_1$  preexponential factors are subject to the optimization. However, because  $m_k$ 's can only take an even integer values, their optimization is done only once and is based on a stochastic search with a predefined number of trials. The probability density from which the  $L_k$  and  $m_k$  parameters of new random candidate functions are sampled is based on the distribution of these parameters in the existing basis. After the stochastic trials of random candidate functions are complete, the one that lowers the energy the most is included in the basis. The range of allowed values for  $m_k$ 's is set to 0–200. After a certain number of Gaussians are added, the nonlinear parameters of all functions in the basis set generated so far are reoptimized, again using a one-

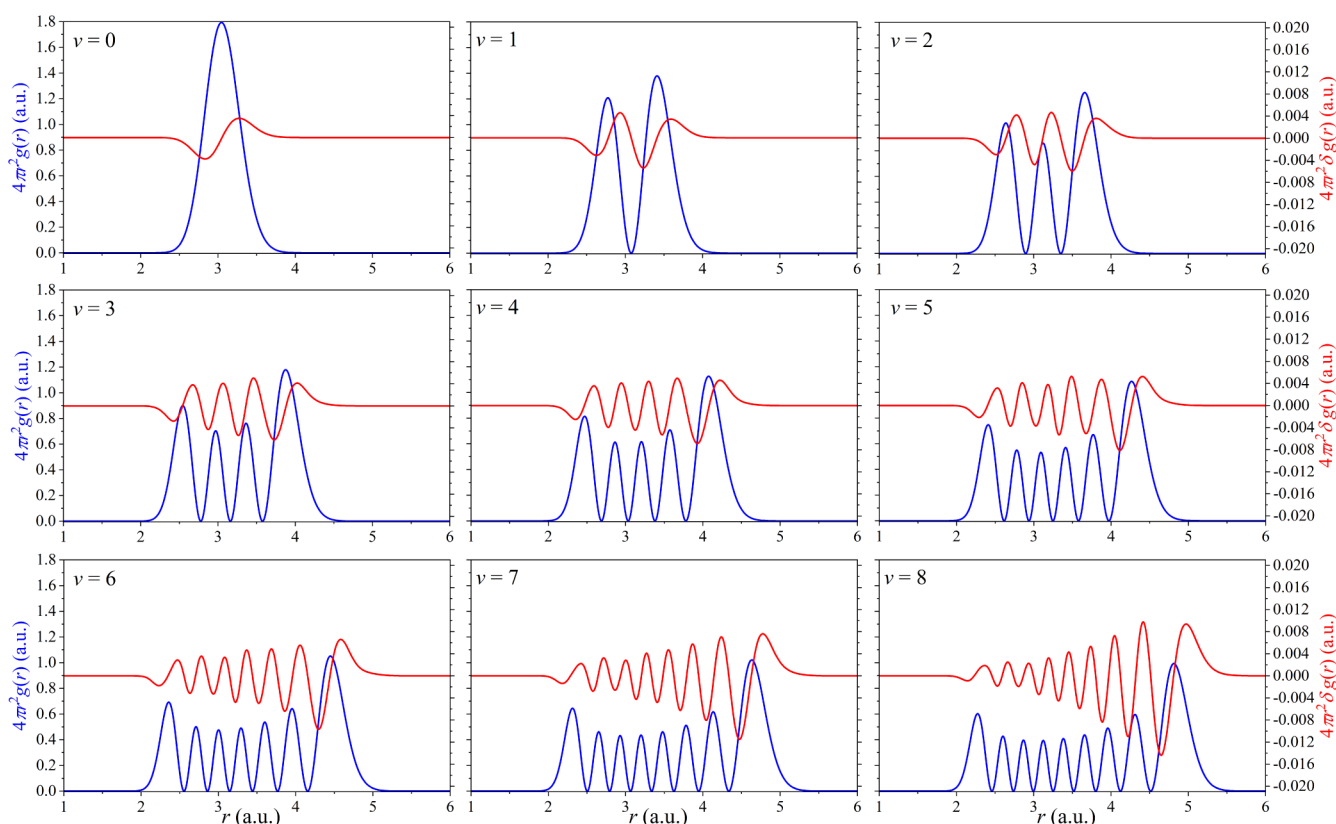


**Figure 1.** Nucleus–nucleus pair correlation functions,  $g$ , of LiH calculated using the non-BO wave functions obtained with the largest basis sets of 17 000 ECGs in this work along with the difference,  $\delta g = g_{\text{Li-H}}^{\text{non-BO}} - g_{\text{Li-H}}^{\text{BO}}$ , with respect to the square of the corresponding vibrational wave functions obtained in BO ECG calculations. Each point of the BO potential energy curve calculated with 2400 ECGs has been taken from ref. 28 Note that the scale for  $g$  is shown on the left vertical axis, while the scale for  $\delta g$  is given on the right vertical axis.

function-at-a-time approach. In this reoptimization, however, only the  $L_k$  matrix elements are varied, while the  $m_k$  values are kept unchanged. At the largest basis set size of 17 000 used in the present work, several additional reoptimization cycles are performed, which further lowered the nonrelativistic energies. This is the reason why some of the energy gains going from 15 000 to 17 000 function basis sets in Table 1 are larger than those that correspond to the difference between the 13 000 to 15 000 function basis sets.

The vibrational transition energies calculated using the nonrelativistic non-BO energies ( $E_{\text{nr}}$ ), nonrelativistic non-BO energies plus leading relativistic corrections ( $E_{\text{nr+rel}}$ ), and nonrelativistic non-BO energies plus leading relativistic and QED corrections ( $E_{\text{nr+rel+QED}}$ ) are shown in Table 2. In addition to the non-BO values calculated in the present work, some most accurate values obtained in previous experimental studies and theoretical BO calculations are also shown in the table. All of the previous calculations,<sup>28,49,50</sup> have been performed assuming the BO approximation; although, adiabatic correction has been included in the calculations performed by Holka et al.<sup>50</sup> and Tung et al.,<sup>28</sup> which makes their values more accurate than those obtained in other studies and more directly comparable to the present work. It should be noted that of the three referenced BO calculations, only those by Tung et al.<sup>28</sup> show good agreement with experimental transition energies.

As can be seen in Table 2, the values obtained in this study, are the most accurate theoretical values ever reported for the lowest three states. For instance, the value of 1 359.725(53)  $\text{cm}^{-1}$  obtained in the present work for the  $\nu = 0 \rightarrow \nu = 1$  transition,

is in excellent agreement with the values of 1 359.71(2)<sup>51</sup> and 1359.708 5(20)<sup>52</sup> derived from the experimental data. Although 17 000 ECGs have been used in the wave function expansion for all considered states, the accuracy of the obtained transition energies decreases with increasing the excitation level. Specifically, in the case of the  $\nu = 8 \rightarrow \nu = 7$  transition (the highest two states we studied), the difference between the calculated transition energy of 1 064.5(28)  $\text{cm}^{-1}$  in this work and the experimental values of 1 061.78(2)<sup>51</sup> and 1 061.76(15)<sup>52</sup> are relatively large. This clearly indicates that one must employ an even large number of ECGs than 17 000 in the wave function expansion and/or increase the number of cycles optimizing the nonlinear parameters of the Gaussians to alleviate the error. Furthermore, a comparison of the transition energy values obtained in the ECG calculations with and without assuming the BO approximation reveals the importance of accounting for the coupling between the motion of the electrons and the nuclei. As shown by Holka et al.<sup>50</sup> and confirmed by the present study, the nonadiabatic effects are important to account for even for the fundamental vibrational transition of the LiH molecule if one aims at spectroscopic accuracy in the calculations.

The nonrelativistic non-BO wave functions obtained for LiH with the largest basis sets for the studied states were used to calculate the expectation values of the interparticle distances and their squares. The mean values of the Dirac delta functions dependent on interparticle distances were also computed. The results are shown in Table 3. Additionally, the table includes the equilibrium bond lengths,  $r_e$ , and the vibrationally averaged

bond lengths,  $\langle r_{\text{Li-H}} \rangle$ , obtained in BO calculations. One may notice that one of the experimental  $r_e$  values (3.013 946 40 au from ref. 54 does not match the other two (3.015 217 in ref. 51 and 3.015 235 97 in ref. 52). As our present non-BO calculations explicitly account for the coupling between the electron and nuclear motions, it is expected that the results should exhibit some small difference when compared to the corresponding expectation values obtained in BO calculations. This is indeed the case. For example, the difference in the  $\langle r_{\text{Li-H}} \rangle$  value (3.061 036 85(61) bohr vs 3.060 291 88 bohr) occurs in the fourth decimal figure. Similar differences were also found before in the studies that accounted for the adiabatic and nonadiabatic effects in the calculations of properties of diatomic molecules.<sup>50</sup>

Lastly, in Figure 1 we show the nucleus–nucleus pair correlation functions, defined as  $g(\xi) = \langle \delta(r_1 - \xi) \rangle$ , computed for all considered states of LiH using the largest basis sets of 17 000 ECGs generated in this work. It should be noted that in the limit of the infinite nuclear mass, the non-BO nucleus–nucleus correlation function becomes equal to the square of the vibrational wave function in the BO calculations, i.e., these two distributions are closely related. Therefore, in order to highlight the difference between them, in Figure 1 we also show  $g_{\text{Li-H}}^{\text{non-BO}} - g_{\text{Li-H}}^{\text{BO}}$  (where  $g_{\text{Li-H}}^{\text{BO}}$  is given by the square of the corresponding vibrational wave function) for each state. As expected, the difference (red curve) grows in magnitude with the increase of the vibrational quantum number. Also, the shape and oscillations of the difference indicate that  $g_{\text{Li-H}}^{\text{non-BO}}$  is very slightly shifted overall to the right (i.e., larger values of the internuclear distance) with respect to  $g_{\text{Li-H}}^{\text{BO}}$ . That said, for all considered states, the amplitude of the difference remains rather small in relative terms, that is  $g_{\text{Li-H}}^{\text{non-BO}}$  and  $g_{\text{Li-H}}^{\text{BO}}$  would be hardly distinguishable if plotted side by side. This correlates with our previous findings for the HD<sup>+</sup> molecular ion, where only for the highest 1–2 rovibrational states ( $v = 21, 22$ ), where a dramatic breakdown of the Born–Oppenheimer occurs, one observes a visible mismatch between the nucleus–nucleus correlation functions obtained in calculations with and without the BO approximation.<sup>55</sup>

## CONCLUSION

This work reports non-Born–Oppenheimer variational calculations for the LiH molecule in its ground and the lowest eight vibrationally excited states. The calculations utilize all-particle explicitly correlated Gaussian basis functions. Extensive optimization of the nonlinear parameters of the Gaussians is performed separately for each state, with basis sets expanded to include up to 17 000 functions. The nonrelativistic non-BO wave functions are then used to calculate the leading relativistic and quantum electrodynamics (QED) corrections, which are added to the non-BO nonrelativistic energies. The corrected energies are used to calculate the transition energies between adjacent states. The results obtained for the lowest three states represent the most accurate theoretical values (regardless of the method used) ever computed for the LiH molecule and provide a useful benchmark for future theoretical studies. The corresponding transition energies are in very good agreement with experimental values. The accuracy is gradually decreased for higher vibrationally excited states, where the non-BO calculations are currently behind what is achievable with high-level ECG approaches that resort to the Born–Oppenheimer

approximation. Further improvements on the theoretical side will necessitate the use of larger Gaussian sets and inclusion of higher order relativistic and QED effects. We hope this work will also motivate new spectroscopic measurements of the lithium hydride molecule.

## ASSOCIATED CONTENT

### Supporting Information

The Supporting Information is available free of charge at <https://pubs.acs.org/doi/10.1021/acs.jpca.4c04510>.

The nonlinear parameters of the largest basis sets (17 000 ECGs) employed in this work for all considered states ( $v = 0, \dots, 8$ ) (ZIP)

## AUTHOR INFORMATION

### Corresponding Authors

Saeed Nasiri – Department of Physics, Nazarbayev University, Astana 010000, Kazakhstan; Email: [s.t.nasiri@gmail.com](mailto:s.t.nasiri@gmail.com)

Sergiy Bubin – Department of Physics, Nazarbayev University, Astana 010000, Kazakhstan; Email: [sergiy.bubin@nu.edu.kz](mailto:sergiy.bubin@nu.edu.kz)

Monika Stanke – Institute of Physics, Faculty of Physics, Astronomy, and Informatics, Nicolaus Copernicus University, Toruń PL 87-100, Poland; Email: [monika@fizyka.umk.pl](mailto:monika@fizyka.umk.pl)

Ludwik Adamowicz – Department of Chemistry and Biochemistry and Department of Physics, University of Arizona, Tucson, Arizona 85721, United States; [orcid.org/0000-0001-9557-0484](https://orcid.org/0000-0001-9557-0484); Email: [ludwik@arizona.edu](mailto:ludwik@arizona.edu)

Complete contact information is available at: <https://pubs.acs.org/10.1021/acs.jpca.4c04510>

### Notes

The authors declare no competing financial interest.

## ACKNOWLEDGMENTS

This work has been supported by the National Science Foundation (grant No. 1856702) and Nazarbayev University (faculty development grant No. 021220FD3651). Authors acknowledge the use of the computational resources at the University of Arizona High Performance Computing and the Nazarbayev University Research Computing,

## REFERENCES

- (1) Oliphant, N.; Adamowicz, L. Coupled-cluster method truncated at quadruples. *J. Chem. Phys.* **1991**, *95*, 6645–6651.
- (2) Oliphant, N.; Adamowicz, L. Multireference coupled-cluster method using a single-reference formalism. *J. Chem. Phys.* **1991**, *94*, 1229–1235.
- (3) Oliphant, N.; Adamowicz, L. Multireference coupled cluster method for electronic structure of molecules. *Int. Rev. Phys. Chem.* **1993**, *12*, 339–362.
- (4) Piecuch, P.; Oliphant, N.; Adamowicz, L. A state-selective multireference coupled-cluster theory employing the single-reference formalism. *J. Chem. Phys.* **1993**, *99*, 1875–1900.
- (5) Adamowicz, L.; McCullough, E. A. J. Numerical multiconfiguration self-consistent-field calculations on the first excited state of lithium hydride anion (LiH<sup>-</sup>). *J. Phys. Chem.* **1984**, *88*, 2045–2048.
- (6) Adamowicz, L.; Bartlett, R. J.; McCullough, E. A. Towards Numerical Solutions of the Schrödinger Equation for Diatomic Molecules. *Phys. Rev. Lett.* **1985**, *54*, 426–429.
- (7) Oliphant, N.; Adamowicz, L. Coupled cluster calculations for the BC molecule using numerical correlation orbitals. *Chem. Phys. Lett.* **1990**, *168*, 126–130.



- (8) Adamowicz, L.; Bartlett, R. Very accurate correlated calculations on diatomic molecules with numerical orbitals: The hydrogen fluoride molecule. *Phys. Rev. A* **1988**, *37*, 1–5.
- (9) Adamowicz, L.; Bartlett, R. MBPT and coupled cluster calculation on the neon atom with numerical orbitals. *Int. J. Quantum Chem.* **1987**, *31*, 173–177.
- (10) Adamowicz, L.; Bartlett, R. Accurate numerical orbital MBPT/CC study of the electron affinity of fluorine and the dissociation energy of hydrogen fluoride. *J. Chem. Phys.* **1986**, *84*, 6837–6839.
- (11) Adamowicz, L.; Bartlett, R. Coupled cluster calculations with numerical orbitals for excited states of polar anions. *J. Chem. Phys.* **1985**, *83*, 6268–6279.
- (12) Adamowicz, L. Optimized virtual orbital space (OVOS) in coupled-cluster calculations. *Mol. Phys.* **2010**, *108* (21–23), 3105–3112.
- (13) Les, A.; Adamowicz, L.; Bartlett, R. Relative stability of cytosine tautomers with the coupled cluster method and first-order correlation orbitals. *J. Phys. Chem.* **1989**, *93*, 4001–4005.
- (14) Adamowicz, L. NNO-HCN complex. Ab initio calculations with the coupled cluster method and 1st-order correlation orbitals. *Chem. Phys.* **1992**, *165*, 281–286.
- (15) Adamowicz, L. C<sub>2</sub>H<sub>2</sub>-CO complex. Ab initio calculations with the coupled-cluster method and first-order correlation orbitals. *Chem. Phys. Lett.* **1992**, *192*, 199–204.
- (16) Adamowicz, L. Stable and metastable states of the Si<sub>5</sub><sup>-</sup> anion. Theoretical study. *Chem. Phys. Lett.* **1992**, *188*, 131–134.
- (17) Adamowicz, L. Photoexcitations of the Si<sub>4</sub><sup>-</sup> anion. Theoretical study. *Chem. Phys. Lett.* **1991**, *185*, 244–250.
- (18) Adamowicz, L. Theoretical study of optical excitations of linear C<sub>4</sub><sup>-</sup>. *Chem. Phys.* **1991**, *156*, 387–394.
- (19) Adamowicz, L. Stable and metastable photoexcitations of linear C<sub>6</sub><sup>-</sup>. Theoretical study. *Chem. Phys. Lett.* **1991**, *182*, 45–50.
- (20) Adamowicz, L. Electron affinities of small linear carbon clusters. Coupled cluster calculations with first-order correlation orbitals. *J. Chem. Phys.* **1991**, *94*, 1241–1246.
- (21) Adamowicz, L. NNO-HCl complex. Ab initio calculations with the coupled cluster method and first-order correlation orbitals. *Chem. Phys. Lett.* **1991**, *176*, 249–254.
- (22) Les, A.; Adamowicz, L. First-order correlation orbitals for the MCSCF zeroth-order wave function. *Chem. Phys. Lett.* **1991**, *183*, 483–490.
- (23) Adamowicz, L. Optimized second-order correlation orbital manifold for single excitations in the coupled-cluster method. *Int. J. Quantum Chem.* **1991**, *40*, 71–80.
- (24) Kinghorn, D. B.; Adamowicz, L. Improved Nonadiabatic Ground-State Energy Upper Bound for Dihydrogen. *Phys. Rev. Lett.* **1999**, *83*, 2541–2543.
- (25) Kinghorn, D. B.; Adamowicz, L. A correlated basis set for nonadiabatic energy calculations on diatomic molecules. *J. Chem. Phys.* **1999**, *110*, 7166–7175.
- (26) Scheu, C. E.; Kinghorn, D. B.; Adamowicz, L. Non-Born–Oppenheimer calculations on the LiH molecule with explicitly correlated Gaussian functions. *J. Chem. Phys.* **2001**, *114*, 3393–3397.
- (27) Gilmore, D. W.; Kozłowski, P. M.; Kinghorn, D. B.; Adamowicz, L. Analytic first derivatives for explicitly correlated, multicenter, Gaussian geminals. *Int. J. Quantum Chem.* **1997**, *63*, 991–999.
- (28) Tung, W.-C.; Pavanello, M.; Adamowicz, L. Very accurate potential energy curve of the LiH molecule. *J. Chem. Phys.* **2011**, *134* (6), 064117.
- (29) Strasburger, K.; Ciosłowski, J. Partial-wave decomposition of the one-electron properties of the LiH molecule computed with explicitly correlated basis sets. *Mol. Phys.* **2022**, *120* (19–20), No. e2048107.
- (30) Palikot, E.; Stanke, M.; Adamowicz, L. An algorithm for calculating the Bethe logarithm for small molecules with all-electron explicitly correlated Gaussian functions. *Chem. Phys. Lett.* **2020**, *757*, 137859.
- (31) Nasiri, S.; Shomenov, T.; Bubin, S.; Adamowicz, L. Dissociation energy and the lowest vibrational transition in LiH without assuming the non-Born–Oppenheimer approximation. *Mol. Phys.* **2022**, *120* (24), No. e2147105.
- (32) Nasiri, S.; Adamowicz, L.; Bubin, S. Electron affinity of LiH. *Mol. Phys.* **2022**, *120* (19–20), No. e2065375.
- (33) Bubin, S.; Adamowicz, L.; Molski, M. An accurate non-Born–Oppenheimer calculation of the first purely vibrational transition in LiH molecule. *J. Chem. Phys.* **2005**, *123* (13), 134310.
- (34) Wang, M.; Huang, W.; Kondev, F.; Audi, G.; Naimi, S. The AME 2020 atomic mass evaluation (II). Tables, graphs and references. *Chin. Phys. C* **2021**, *45*, 030003.
- (35) Bubin, S.; Pavanello, M.; Tung, W.-C.; Sharkey, K. L.; Adamowicz, L. Born–Oppenheimer and Non-Born–Oppenheimer, Atomic and Molecular Calculations with Explicitly Correlated Gaussians. *Chem. Rev.* **2013**, *113*, 36–79.
- (36) Matsen, F. A.; Pauncz, R. *The Unitary Group in Quantum Chemistry*; Elsevier: Amsterdam, 1986.
- (37) Pauncz, R. *Spin Eigenfunctions*; Plenum: New York, 1979.
- (38) Hamermesh, M. *Group Theory and Its Application to Physical Problems*; Addison-Wesley: Reading, MA, 1962.
- (39) Caswell, W. E.; Lepage, G. P. Effective lagrangians for bound state problems in QED, QCD, and other field theories. *Phys. Lett. B* **1986**, *167* (4), 437–442.
- (40) Pachucki, K. Effective Hamiltonian approach to the bound state: Positronium hyperfine structure. *Phys. Rev. A* **1997**, *56*, 297–304.
- (41) Bethe, H. A.; Salpeter, E. E. *Quantum Mechanics of One- and Two-Electron Atoms*; Plenum: New York, 1977.
- (42) Akhiezer, A. I.; Berestetskii, V. B. *Quantum Electrodynamics*; John Wiley & Sons: New York, 1965.
- (43) Bubin, S.; Stanke, M.; Molski, M.; Adamowicz, L. Accurate non-Born–Oppenheimer calculations of the lowest vibrational energies of D<sub>2</sub> and T<sub>2</sub> with including relativistic corrections. *Chem. Phys. Lett.* **2010**, *494* (1–3), 21–25.
- (44) Pachucki, K.; Komasa, J. Bethe logarithm for the lithium atom from exponentially correlated Gaussian functions. *Phys. Rev. A* **2003**, *68*, 042507.
- (45) Pachucki, K.; Komasa, J. Relativistic and QED Corrections for the Beryllium Atom. *Phys. Rev. Lett.* **2004**, *92*, 213001.
- (46) Wang, L. M.; Li, C.; Yan, Z.-C.; Drake, G. W. F. Isotope shifts and transition frequencies for the S and P states of lithium: Bethe logarithms and second-order relativistic recoil. *Phys. Rev. A* **2017**, *95*, 032504.
- (47) Drake, G. W. F.; Swainson, R. A. Bethe logarithms for hydrogen up to  $n = 20$ , and approximations for two-electron atoms. *Phys. Rev. A* **1990**, *41*, 1243–1246.
- (48) Hornyák, I.; Nasiri, S.; Bubin, S.; Adamowicz, L. <sup>2</sup>S Rydberg spectrum of the boron atom. *Phys. Rev. A* **2021**, *104*, 032809.
- (49) Lundsgaard, M. F. V.; Rudolph, H. Vibrationally resolved cross sections for single-photon ionization of LiH. *J. Chem. Phys.* **1999**, *111*, 6724.
- (50) Holka, F.; Szalay, P. G.; Fremont, J.; Rey, M.; Peterson, K. A.; Tyuterev, V. G. Accurate ab initio determination of the adiabatic potential energy function and the Born–Oppenheimer breakdown corrections for the electronic ground state of LiH isotopologues. *J. Chem. Phys.* **2011**, *134* (9), 094306.
- (51) Stwalley, W. C.; Zemke, W. T. Spectroscopy and Structure of the Lithium Hydride Diatomic Molecules and Ions. *J. Phys. Chem. Ref. Data* **1993**, *22*, 87–112.
- (52) Coxon, J. A.; Dickinson, C. S. Application of direct potential fitting to line position data for the X<sup>1</sup>Σ<sup>+</sup>A<sup>1</sup>Σ<sup>+</sup> states of LiH. *J. Chem. Phys.* **2004**, *121*, 9378–9388.
- (53) Chang, D. T.; Reimann, K.; Surratt, G.; Gellene, G. I.; Lin, P.; Lucchese, R. R. First principles determination of the photoelectron spectrum of LiH<sup>-</sup>. *J. Chem. Phys.* **2002**, *117*, S757–S763.
- (54) Watson, J. K. G. The inversion of diatomic Born–Oppenheimer-breakdown corrections. *J. Mol. Spectrosc.* **2004**, *223*, 39–50.
- (55) Nasiri, S.; Bubin, S.; Adamowicz, L. Charge asymmetry in HD<sup>+</sup> ion and HD molecule. In *Presented at the American Physical Society March Meeting 2023, Las Vegas, Nevada, March 7, 2023. Session F59.00013*; APS, 2023.